Carbohydrate Polymers 110 (2014) 142–147

Contents lists available at ScienceDirect

Carbohydrate Polymers

journal homepage: www.elsevier.com/locate/carbpol

A glucan isolated from flowers of *Lonicera japonica* Thunb. inhibits aggregation and neurotoxicity of Aβ_{42}

Peipei Wang[a,c,1], Wenfeng Liao[a,1], Jianping Fang[a], Qin Liu[a], Jian Yao[a], Minghua Hu[b], Kan Ding[a,*]

[a] *Glycochemistry & Glycobiology Lab, Shanghai Institute of Materia Medica, Chinese Academy of Sciences, Shanghai 201203, China*
[b] *Infinitus Co., Ltd, Guangzhou 510623, China*
[c] *State Key Laboratory of Natural Medicines, China Pharmaceutical University, Nanjing 210009, China*

ARTICLE INFO

Article history:
Received 29 December 2013
Received in revised form 10 March 2014
Accepted 17 March 2014
Available online 31 March 2014

Keywords:
Lonicera japonica Thunb.
Aβ_{42}
Glucan
Aggregation and neurotoxicity
Alzheimer's disease

ABSTRACT

Inhibition of Aβ aggregation and attenuation of its cytotoxicity are considered to valuable therapeutics for Alzheimer's disease (AD). Here, a glucan named as LJW0F2 was purified from flowers of *Lonicera japonica* Thunb. Using monosaccharides composition analysis, methylation analysis, IR and NMR spectroscopy, this polysaccharide was elucidated to be an α-D-(1→4)-glucan with an α-(1→4) linked branch attached to the C-6 position. Its inhibitory effect on Aβ_{42} aggregation was measured by fluorescence spectroscopic analysis with thioflavine T (ThT) and atomic force microscopy (AFM). We showed that polysaccharide LJW0F2 could inhibit Aβ_{42} aggregation in a dose-dependent-manner. Besides, LJW0F2 could attenuate the cytotoxicity induced by Aβ_{42} aggregation in SH-SY5Y neuroblastoma cells. To the best of our knowledge, this was the first report that the exogenous plant-derived polysaccharide might block Aβ_{42} aggregation directly and reduce its toxicity in SH-SY5Y cells.

© 2014 Elsevier Ltd. All rights reserved.

1. Introduction

Alzheimer's disease (AD) is a progressive neurodegenerative disease, which leads to cognitive dysfunction and neuronal death. The prevalence of AD induces great pressure on the social and health-care systems of aging population's society (Dartigues, 2009; Nathalie & Jean-Noel, 2008; Wimo, Winblad, & Jonsson, 2010). There is an unmet need for therapies which can arrest or reverse AD progression, due to current treatments of AD only for alleviating the symptoms (Gerald & Ockert, 2012). To date, numerous hypotheses were proposed to understand the molecular mechanisms of the pathogenesis of AD, while one of the most recognized one was the "amyloid hypotheses" (Prasansuklab & Tencomnao, 2013). It is believed that the neuropathogenesis of AD may be triggered by the accumulation of misfolded Aβ in the central nervous system (Goedert & Spillantini, 2006; Ittner & Gotz, 2011).

The monomeric Aβ is a 39–42 residue peptide, derived from the intracellular cleavage of amyloid precursor protein by the sequential hydrolysis of two proteolytic enzymes, β-secretase and γ-secretase (Nathalie & Jean-Noel, 2008; Selkoe, 1997). Actually, soluble monomeric Aβ peptides are normally produced in the brain, but they can self-aggregate into various sized oligomers and insoluble fibrils and further subsequently form neuritic plaques due to its overproduction or defective clearance (Englund et al., 2007; Lesne et al., 2006; Liu et al., 2011; Matveeva, Rudolph, Moll, & Thompson, 2012). Existing data have proposed to explain how the accumulation of Aβ exert a cascade of harmful events rated to AD by triggering inflammatory responses (Salminen, Ojala, Kauppinen, Kaarniranta, & Suuronen, 2009), oxidative damage (Yankner, 1996), dysregulation of Ca^{2+} ion homeostasis (Demuro et al., 2005; Yankner, 1996), and altered kinase and phosphatase activities that can lead to neurofibrillary tangles (Busciglio, Lorenzo, Yeh, & Yankner, 1995; Tseng, Green, Chan, Blurton-Jones, & LaFerla, 2008; Zheng, Bastianetto, Mennicken, Ma, & Kar, 2002). More recent evidences suggested that the soluble oligomers were more toxic *in vitro* and *in vivo* than fibrils, and might represent the primary pathological species of AD (Benilova, Karran, & De Strooper, 2012; Cleary et al., 2005; Ono, Condron, & Teplow, 2009). Therefore, inhibition of Aβ accumulation and attenuation of its neurotoxcity are thought to be effective strategies for the prevention and/or treatment of AD.

Several polysaccharides extracted from traditional Chinese herbs have been reported to have neuroprotective effects *in vitro*, possibly due to their antioxidant activity, such as polysaccharide

* Corresponding author at: 555 Zu Chong Zhi Road, Pudong, Shanghai 201203, China. Tel.: +86 21 50806928; fax: +86 21 50806928.
E-mail address: dingkan@simm.ac.cn (K. Ding).
[1] These two authors contributed equally to this work.

http://dx.doi.org/10.1016/j.carbpol.2014.03.060
0144-8617/© 2014 Elsevier Ltd. All rights reserved.

extracted from *Lycium barbarum* (Ho et al., 2010) and polysaccharide PS5 from *Rubia cordifolia* (Chakrabortee et al., 2012).

Lonicera japonica Thunb., is an important traditional Chinese herbal medicine which has been used to treat fever, headache and some infection diseases for thousands years. Many biological activities of this herb have been reported, such as antioxidative, aninflammatory, antibacterial, antiviral and hepatoprotective activities (Shang, Pan, Li, Miao, & Ding, 2011). Recently, a crude water extract from flowers of *L. japonica* Thunb. was shown to have neuroprotective effects in human neuroblastoma cells (SH-SY5Y) (Kwon et al., 2011). However, the active substance and underling mechanism of its protective effects were not known clearly. In the present study, we firstly reported the structure of a glucan named as LJW0F2 from flowers of *L. japonica* Thunb. The inhibitory effects of this polysaccharide on aggregation and neurotoxicity of Aβ_{42} were also evaluated.

2. Materials and methods

2.1. Materials

The dried flowers of *L. japonica* Thunb. were purchased from the local market (Hujiyutang Co., Ltd., Shanghai, China) and were identified by Prof. Ping Li (Department of Pharmacognosy, China Pharmaceutical University, Nanjing, China). DEAE-Cellulose 32 was from Whatman Co., U.K. Sephadex G-150 was from Amersham Bioscience, USA. Monosaccharide standards were all from Fluka, Switzerland. Trifluoroacetic acid (TFA), thioflavine-T (ThT) and 1-phenyl-3-methyl-5-pyrazolone (PMP) were from Sigma–Aldrich, USA. Dextran standards were purchased from Pharmacia Co., Sweden. Acetonitrile and dimethyl sulfoxide (DMSO) were purchased from E. Merck, Germany. Beta amyloid peptide 42 (Aβ_{42}), Ultra Pure, HFIP was purchased from rPeptide, USA. The cell counting kit-8 (CCK-8) was purchased from Dojindo Laboratories (Kumamoto, Japan). Other reagents were of analytical grade(Sinopharm Chemical Reagent Co., Ltd, China).

2.2. General analysis

Total sugar content was determined by the phenol–sulfuric acid method using glucose as standard (Dubois, Gilles, Hamilton, Rebers, & Smith, 1956). The content of protein was determined by the Lowry method (Lowry, Rosebrough, Farr, & Randall, 1951). Uronic acid was determined by m-hydroxyl diphenyl method (Blumencrantz and Asboe-Hansen, 1973), and glucuronic acid was employed as standard control.

2.3. Extraction, isolation and purification of polysaccharides

Extraction of crude polysaccharides was performed by the previous procedure (Chen et al., 2011). In brief, the dried flowers of *L. japonica* Thunb. (5.0 kg) was defatted with 95% EtOH for two weeks and then extracted with boiling water for five times, 5 h for each time. The combined supernatant was concentrated and treated with 15% trichloroacetic acid at 4 °C for 4 h to remove the protein. After neutralization and centrifugation, the supernatant was dialyzed (molecular weight cut-off 3500 Da). Three volumes of 95% EtOH were added to the concentrated retentate to precipitate the crude polysaccharide, LJW (325 g, 6.5%). LJW (8 g) was fractionated on a DEAE-cellulose column (Cl^-, 120 cm × 6 cm), eluted with distilled water to obtain the fraction LJW0. Then, the polysaccharide LJW0 was further purified on a Sephadex G150 column (2.6 cm × 100 cm), eluted with 0.2 M NaCl, to obtain the polysaccharide LJW0F2. The eluate was monitored with a phenol–sulfuric acid method.

2.4. Homogeneity and molecular weight

The homogeneity and relative molecular weight of polysaccharide LJW0F2 were determined by high performance gel permeation chromatography (HPGPC) with series-connected Ultrahydrogel TM 2000 and Ultrahydrogel TM 500 columns on an Agilent 1200 instrument (Chen et al., 2011). For molecular weight estimation, the columns were calibrated by standard T-series Dextrans with different molecular weight. Data were analyzed by GPC software.

2.5. Monosaccharide composition analysis

Monosaccharide composition of LJW0F2 was determined by a HPLC method according to previous report (Wang et al., 2012). Briefly, LJW0F2 was totally hydrolyzed with 2 M TFA at 110 °C for 4 h. The monosaccharides released were derivatived with PMP and then analyzed by HPLC on a XDB-C_{18} column eluted with acetonitrile/phosphate buffer solution (18:82, pH 6.7) at a flow rate of 1.0 mL/min. The detective ultraviolet wavelength was set at 254 nm. The composition and content of monosaccharides were determined by comparing retention times and peak areas of the tested residues, with that of monosaccharide standards (mannose, arabinose, xylose, galactose and glucose), respectively.

2.6. Methylation analysis

The vacuum-dried polysaccharide LJW0F2 (10 mg) was methylated for three times based on previous methods (Hakomori, 1964). The completeness of methylation was confirmed by the disappearance of the hydroxyl absorption in IR spectrum (Nujol). The methylated polysaccharide was hydrolyzed with 2 M TFA at 110 °C for 2 h and then reduced with sodium borohydride and acetylated. The partially methylated alditol acetates were analyzed by Gas chromatography–mass spectrometry (GC–MS) with a Shimadzu QP-5050A apparatus equipped with a DB-1 capillary column (0.25 mm × 30 m). Mass spectra of the derivatives were analyzed using Complex Carbohydrate Structural Database of Complex Carbohydrate Research Centre (http://www.ccrc.uga.edu/).

2.7. FTIR and NMR analysis

Polysaccharides were ground with KBr powder (native polysaccharide) or Nujol film (permethylated polysaccharide) and pressed into pellets for FT-IR measurement (PerkinElmer 591B, USA) in the frequency range of 4000–500 cm^{-1}.

For NMR analysis, the polysaccharide LJW0F2 (30 mg) was exchanged and dissolved in 0.5 mL of D_2O. The ^1H NMR, ^{13}C NMR spectra, two-dimensional COSY, HSQC and HMBC spectra were measured at room temperature with acetone as internal standard. NMR spectra were recorded on a Varian Mercury 500 MHz spectrometer.

2.8. Thioflavine T fluorescence assay

The freshly prepared Aβ_{42} (2 mM in DMSO) was diluted to a final concentration of 20 μM in 20 μL of fibril-formation buffer (50 mM sodium phosphate, pH 7.5, 100 mM NaCl and 0.02% NaN_3), with or without polysaccharides LJW0F2, in a 96-well plate. After the resulting mixture were pre-incubated for 30 min at room temperature, 80 μL of ThT solution (6.25 μM in 50 mM glycine–NaOH at pH 8.5) was added, shaking at 200 rpm at 37 °C. ThT fluorescence intensity was measured at intervals in a fluorescence plate reader (Novostar, BMG labtech, Germany, EX = 440/10 nm, EM = 483/10 nm) (McKoy, Chen, Schupbach, & Hecht, 2012).

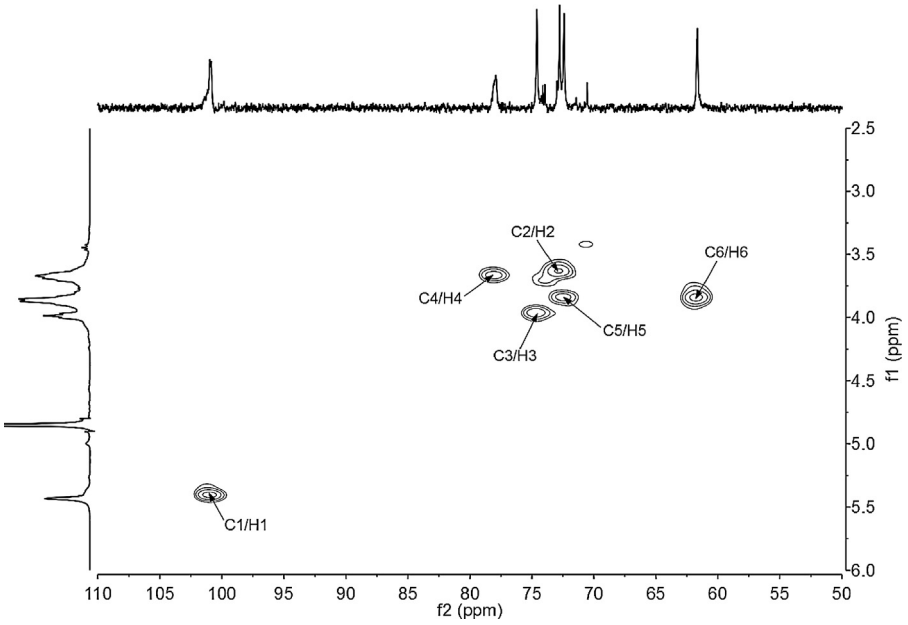

Fig. 1. HSQC spectrum of LJW0F2.

2.9. Atomic force microscope imaging

The procedures of sample preparation for AFM were similar as that for ThT assay. The samples (20 μM $A\beta_{42}$, 100 μL in ultra pure water with 0.02% NaN_3) with or without LJW0F2 were incubated at 37 °C. After 21 d, 5 μL of the sample solution were placed on black mica, dried for 24 h at room temperature, rinsed (100 μL × 6) with ultra-pure water, dried for 10 min under vacuum, then allowed to dry at room temperature prior to examination with AFM. Images were acquired in air using BioScope NanoScope IIIa system (Veeco/Digital Instruments, Santa Barbara, CA, USA) operating in Tapping Mode using silicon probes (Olympus, Tokyo, Japan) (Wada, Miyazawa, & Miura, 2011).

2.10. Cell culture and cell viability assay

SH-SY5Y cells were grown in a minimal essential medium (MEM, Hyclone, USA) and Ham's modification of F-12 (F12, Hyclone, USA, v/v, 1:1), supplemented with 10% fetal bovine serum (FBS, Gibco, USA) and 1% penicillin/streptomycin antibiotics. Cells were cultured at 37 °C in a 5% CO_2 atmosphere. For the cell viability assay, SH-SY5Y cells were seeded at a density of 3.5×10^4 cells/well in 96-well plates. After 24 h, 20 μM of $A\beta_{42}$ either being incubated alone or being co-incubated with LJW0F2 were diluted with fresh medium (MEM/F12, without FBS) and added to each well. The final concentration of $A\beta_{42}$ in each well was 2 μM. Following incubation with cells for 48 h at 37 °C, cell viability was evaluated using CCK-8 assay. Briefly, a 10 μL aliquot of CCK-8 reagent was added to each well and maintained for another 4 h. Absorbance was measured using a spectrophotometer at 450 nm. The cell viability was calculated as Samples/Blank × 100% (Hu et al., 2004).

2.11. Statistic analyses

Data were expressed as mean values ± standard deviation (S.D.). And the data were analyzed by Student *t*-test; *p* values of <0.05 indicated significant differences ($^*p < 0.05$; $^{**}p < 0.01$).

3. Results

3.1. Extraction, purification and composition analysis of polysaccharides

The polysaccharide LJW0F2 was purified by anion-exchange chromatography and gel permeation chromatography. Its homogeneity was estimated by HPGPC, in which it showed one symmetrical peak (Fig. S1, Supplementary data). The relative molecular weight of LJW0F2 was estimated to be 37.1 kDa by comparing with the molecular weight of the standards. The results showed that LJW0F2 contained no protein or uronic acid after the measurement by the Lowry method and m-hydroxyl diphenyl method, respectively. Monosaccharide composition analysis of LJW0F2 was carried out by HPLC following acid hydrolysis and derivatization with PMP. The results indicated that LJW0F2 consisted only of glucose (99.7%).

3.2. FTIR and NMR analysis

The bands on the IR spectrum (figure not shown) of LJW0F2 at 3403.7, 2927.4, and 1643.0 cm^{-1} are assigned to the hydroxyl stretching vibration, C—H stretching vibration and associated water, respectively (Cui et al., 2008). The absorption at 929.2 cm^{-1} is typical signal for D-Glc in the pyranose form (Barker, Bourne, Stacey, & Whiffen, 1954). There was no absorbing signal at 1260 cm^{-1}, indicating that LJW0F2 might contain no sulfated groups. These results suggested that LJW0F2 might be a neutral glucan.

All the chemical shifts of LJW0F2 in the ^{13}C NMR and ^1H NMR spectra were assigned with the help of the COSY (Fig. S2) and HSQC spectrum (Fig. 1). In the ^{13}C NMR spectrum of LJW0F2, only one anomeric resonance signal at δ101.00 (Fig. 1) was present, indicating α-glycosidic linkages, which was confirmed by the broad strong signal at around δ5.40 in the ^1H NMR spectrum (Fig. 1). The signal at δ78.05 was assigned to the substituted C4 of l, 4-linked glucose. The other signals at δ74.68, δ72.87, δ72.45 and δ61.82 were from C3, C2, C5 and C6 of l, 4-linked glucose, respectively. These data were in good agreement with that of the previous literature (Chen et al., 2011). In the HMBC spectrum (Fig. 2), cross peaks of the

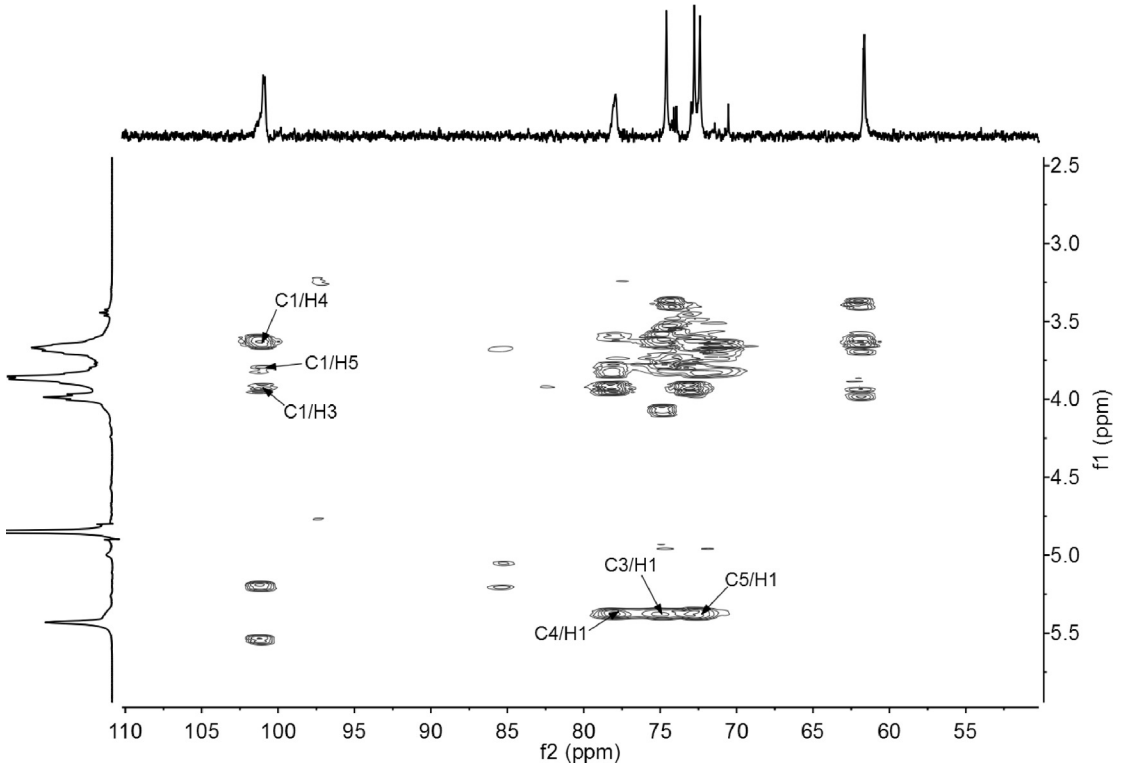

Fig. 2. HMBC spectrum of LJW0F2.

Table 1
Linkage analysis of LJW0F2 by GC–MS.

Methylated residues	Linkages	Molar ratio (%)
2,3,4,6-Me4-Glc*p*	Terminal	5.74
2,3,6-Me3-Glc*p*	1,4-Glc*p*	85.54
2,3-Me2-Glc*p*	1,4,6-Glc*p*	6.39

C1/H3, C1/H4, C1/H5, C3/H1, C4/H1 and C5/H1 were also assigned to confirm the 1,4-linkage in the polysaccharide.

3.3. Linkage analysis

In order to determine the linkage types of LJW0F2, the polysaccharide was per-methylated, hydrolyzed and then the partially methylated alditol acetates (PMAA) were analyzed by GC–MS. The results of methylation analysis were shown in Table 1. The linkages of LJW0F2 consisted of terminal Glucose (T-Glc), 1,4- and 1,4,6-linked glucose, in the molar ratio of 1:14:1.

According to all these data, the full structure of LJW0F2 was proposed as below:

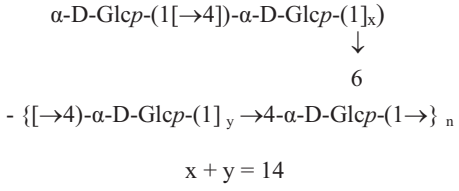

3.4. Inhibitory effects of LJW0F2 on $A\beta_{42}$ aggregation

The ThT dye fluorescence is used regularly to quantify the formation and inhibition of amyloid fibrils in the presence of anti-amyloidogenic compounds. Here, it was used to determine the presence of $A\beta_{42}$ aggregates. When the monomer $A\beta_{42}$ was incubated in PBS buffer (Fig. 3) alone, the fluorescent intensity of ThT was increased in a time dependent manner during the incubation period from 6 h to 24 h. To investigate the inhibitory effects of LJW0F2 on $A\beta_{42}$ aggregation, $A\beta_{42}$ was co-incubated with 50 μg/mL, 100 μg/mL and 200 μg/mL of LJW0F2, respectively. The results showed that the final level of fluorescence of ThT was dramatically decreased in the presence of LJW0F2 with a dose-dependent manner. When $A\beta_{42}$ was co-incubated with 200 μg/mL of LJW0F2, the inhibition ratio was more than 90% over the entire time span compared with that of $A\beta_{42}$ incubation alone (Fig. 3). Although LJW0F2 had little inhibitory effect at the low concentration of 50 μg/mL, it still could delay formation of $A\beta_{42}$ fibrils. Hence, the results suggested that LJW0F2 could impede $A\beta_{42}$ aggregation directly.

The morphological changes of $A\beta_{42}$ aggregation co-incubated with different concentrations of LJW0F2 were examined by AFM. To avoid the confusing effects of iron for AFM images, the PBS buffer was replaced by ultra pure water with 0.02% NaN_3. The results of $A\beta_{42}$ treated with or without LJW0F2 were detected on alternate days. After incubation for 21 d, significant amounts of

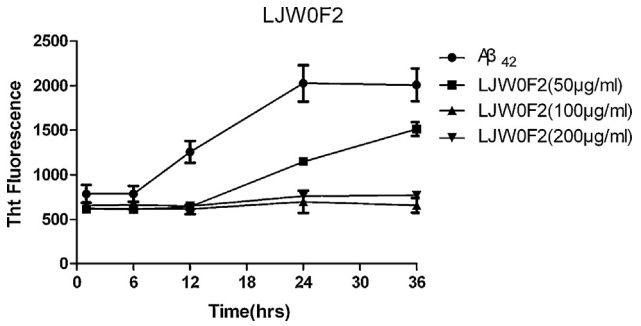

Fig. 3. ThT fluorescence assays. 20 μM $A\beta_{42}$ incubated in the presence of polysaccharide LJW0F2 at different concentrations of 50 μg/mL, 100 μg/mL and 200 μg/mL for 36 h.

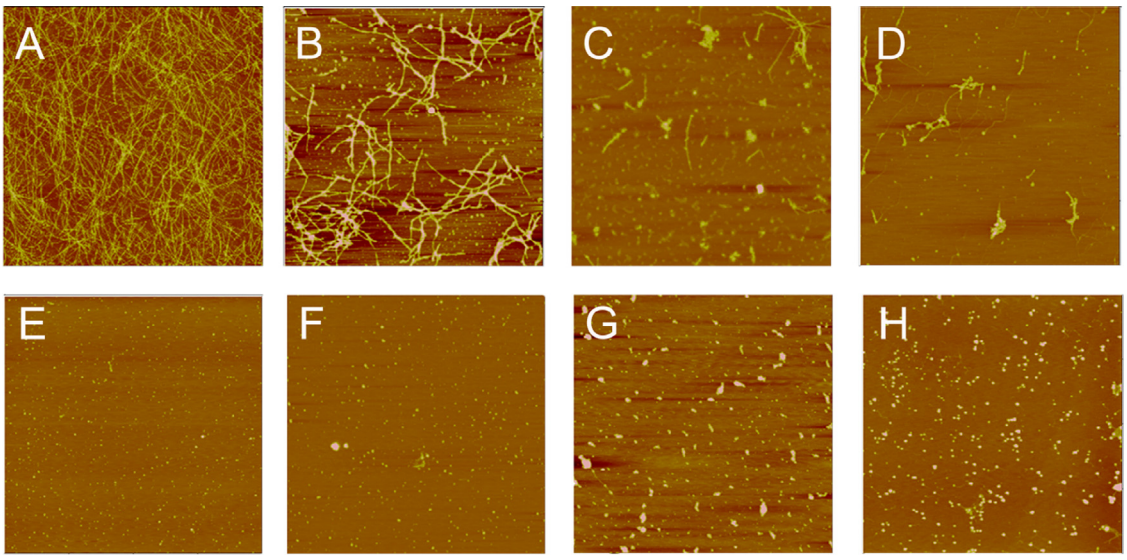

Fig. 4. AFM images of amyloid fibrils formed when Aβ_{42} was incubated alone (A) or in the presence of polysaccharide LJW0F2 at different concentration of 50 μg/mL (B), 100 μg/mL (C) and 200 μg/mL (D) at 37 °C for 21 d, fresh control Aβ_{42} alone (E). As control, the polysaccharide LJW0F2 was incubated alone with three different concentration at 37 °C for 21 d (F–H). The figure size was 10 μm × 10 μm.

fibrils were formed in the 20 μM of Aβ_{42} control group (Fig. 4A). When Aβ_{42} was co-incubated with LJW0F2, the numbers of fibrils observed were decreased dramatically with increasing concentration of LJW0F2, very few fibrils were observed (Fig. 4D), when the treatment concentration of LJW0F2 was at the highest (200 μg/mL). As the concentration of LJW0F2 was decreased, the numbers of fibrils were increased (Fig. 4C). However, the numbers of fibrils were substantially lower than the control group when Aβ_{42} was treated with 50 μg/mL of LJW0F2 (Fig. 4B).

In agreements with ThT staining results, the results of AFM indicated that polysaccharide LJW0F2 could block the fibrils formation of Aβ_{42} directly. It was well known that the formation of Aβ_{42} fibrils was considered as a key step in the pathological progress of AD. Preventing Aβ_{42} aggregation was considered as one of primary therapeutic strategies for treating AD. Up to now, a number of small molecules extracted from traditional Chinese herbal medicine have been shown to be capable of inhibiting Aβ aggregation, such as resveratrol, curcumin, and EGb761 (Chakrabortee et al., 2012; McKoy et al., 2012). However, little studies had mentioned the effects of polysaccharides on Aβ_{42} aggregation, although they were also important bioactive molecules in traditional Chinese herbs. Here, our studies showed that the polysaccharide LJW0F2 could inhibit Aβ_{42} aggregation directly in a dose-dependent manner. Theoretically, the inhibitory mechanism of polysaccharides might be different from that of small molecules. One potential explanation for the mechanism was that the polysaccharide LJW0F2 could form a coating layer around Aβ_{42}, which efficiently competed with Aβ_{42} to form hydrogen bonds with the solvent water molecules, thereby stabling the native conformation of Aβ_{42} and inhibiting Aβ_{42} aggregation (Wada et al., 2011).

3.5. LJW0F2 attenuated neurotoxcity induced by Aβ_{42}

To investigate the neurotoxcity induced by Aβ_{42} *in vitro*, SH-SY5Y cells were exposed to 2 μM Aβ_{42} which was pre-incubated for different time periods (1 d, 2 d, 4 d and 7 d). Then cell viability was detected by CCK-8 assay after 48 h. The results showed that cell viability of SH-SY5Y cells was reduced to different degrees after the treatment with aged Aβ_{42} comparing to Blank group. The ratio of cell viability was reduced to 77.3% after the treatment with 7 d aged Aβ_{42} (Fig. 5A). Hence, 7 d aged Aβ_{42} was used to induce SH-SY5Y cell injury in the subsequent experiment. In order to evaluate the inhibitory effect of LJW0F2 on neurotoxicity induced by aged Aβ_{42}, Aβ_{42} was pre-incubated alone or co-incubated with different concentration of LJW0F2 for 7 d respectively, before they were added to SH-SY5Y cells. As illustrated in Fig. 5B, the results

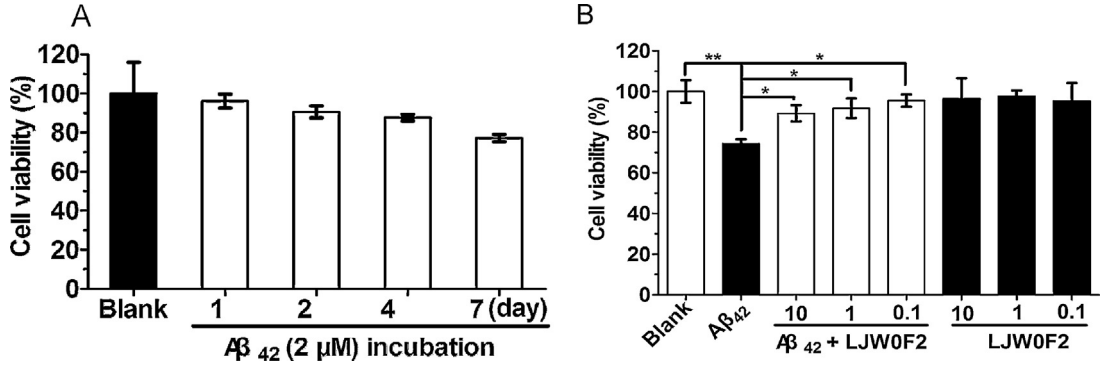

Fig. 5. The results of cell viability assay. Before the SH-SY5Y cells were treated with 2 μM Aβ_{42} for 48 h, the Aβ_{42} had been pre-incubated for 1 d, 2 d, 4 d and 7 d, respectively, then followed by the CCK-8 assay (A). Cell viability assay of SH-SY5Y cells exposed for 48 h to 2 μM Aβ_{42} after the Aβ_{42} pre-incubated for 7 d, either alone or in the presence of polysaccharide LJW0F2 at different concentrations of 0.1 μg/mL, 1 μg/mL and 10 μg/mL. Survival of control cells not exposed to Aβ_{42} was assigned 100% viability. As control, Cell viability assay of SH-SY5Y cells exposed to the polysaccharide LJW0F2 at different concentrations for 48 h was also conducted (B).

showed that LJW0F2 could attenuate Aβ_{42}-induced neurotoxicity in a dose-dependent manner. Notably, LJW0F2 at each of these concentrations alone did not cause any apparent cytotoxicity. Based on the above results, we suggested that the polysaccharide LJW0F2 could attenuate Aβ_{42}-induced neurotoxicity by inhibiting its aggregation. As a major bioactive molecule extracted from flowers of *L. japonica* Thunb., the polysaccharide LJW0F2 showed potential use in treatment of AD.

4. Conclusion

In this study, a neutral glucan, LJW0F2 was purified from the flowers of *L. japonica* Thunb. Its structure was elucidated as an α-D-(1→4)-glucan with an α-(1→4) linked branch attached to C-6 position. Notably, bioactivity tests indicated that LJW0F2 could inhibit Aβ_{42} aggregation directly and attenuate neurotoxicity induced by Aβ_{42} in a dose-dependent manner *in vitro*. Therefore, the molecular mechanism of its inhibitory effect and its potential use in treatment of AD warranted further study.

Acknowledgements

This work was supported by grants from New Drug Creation and Manufacturing Program (2012ZX09301001-003), National Science Fund for Distinguished Young Scholars in China (81125025), National Natural Science Foundation of China (31230022), Industry-University-Research Institute Alliance Fund in Guangdong Province, China (2010A090200041) and Shanghai Research Program (13ZR1447500).

Appendix A. Supplementary data

Supplementary data associated with this article can be found, in the online version, at http://dx.doi.org/10.1016/j.carbpol.2014.03.060.

References

Barker, S. A., Bourne, E. J., Stacey, M., & Whiffen, D. H. (1954). Infra-red spectra of carbohydrates. Part 1. Some derivatives of D-glucopyranose. *Journal of the Chemical Society*, 171–176.

Benilova, I., Karran, E., & De Strooper, B. (2012). The toxic Aβ oligomer and Alzheimer's disease: An emperor in need of clothes. *Nature Neuroscience*, *15*, 349–357.

Blumenkrantz, N., & Asboe-Hansen, G. (1973). New method for quantitativedetermination of uronic acids. *Analytical Biochemistry 54*, 484–489.

Busciglio, J., Lorenzo, A., Yeh, J., & Yankner, B. A. (1995). β-Amyloid fibrils induce tau phosphorylation and loss of microtubule binding. *Neuron*, *14*, 879–888.

Chakrabortee, S., Liu, Y., Zhang, L., Matthews, H. R., Zhang, H., Pan, N., et al. (2012). Macromolecular and small-molecule modulation of intracellular Aβ_{42} aggregation and associated toxicity. *Biochemical Journal*, *442*, 507–515.

Chen, X., Cao, D., Zhou, L., Jin, H., Dong, Q., Yao, J., et al. (2011). Structure of a polysaccharide from *Gastrodia elata* Bl., and oligosaccharides prepared thereof with anti-pancreatic cancer cell growth activities. *Carbohydrate Polymers*, *86*, 1300–1305.

Cleary, J. P., Walsh, D. M., Hofmeister, J. J., Shankar, G. M., Kuskowski, M. A., Selkoe, D. J., et al. (2005). Natural oligomers of the amyloid-β protein specifically disrupt cognitive function. *Nature Neuroscience*, *8*, 79–84.

Cui, H., Liu, Q., Tao, Y., Zhang, H., Zhang, L., & Ding, K. (2008). Structure and chain conformation of a (1→6)-α-D-glucan from the root of *Pueraria lobata* (Willd.) Ohwi and the antioxidant activity of its sulfated derivative. *Carbohydrate Polymers*, *74*, 771–778.

Dartigues, J. F. (2009). Alzheimer's disease: A global challenge for the 21st century. *Lancet Neurology*, *8*, 1082–1083.

Demuro, A., Mina, E., Kayed, R., Milton, S. C., Parker, I., & Glabe, C. G. (2005). Calcium dysregulation and membrane disruption as a ubiquitous neurotoxic mechanism of soluble amyloid oligomers. *Journal of Biological Chemistry*, *280*, 17294–17300.

Dubois, M., Gilles, K. A., Hamilton, J. K., Rebers, P. A., & Smith, F. (1956). Colorimetric method for determination of sugars and related substances. *Analytical Chemistry*, *28*, 350–356.

Englund, H., Sehlin, D., Johansson, A. S., Nilsson, L. N., Gellerfors, P., Paulie, S., et al. (2007). Sensitive ELISA detection of amyloid-beta protofibrils in biological samples. *Journal of Neurochemistry*, *103*, 334–345.

Gerald, Z., & Ockert, W. (2012). Alzheimer's disease market: Hope deferred. *Nature Reviews. Drug Discovery*, *12*, 19–20.

Goedert, M., & Spillantini, M. G. (2006). A century of Alzheimer's disease. *Science*, *314*, 777–781.

Hakomori, S. (1964). A rapid permethylation of glycolipid, and polysaccharide catalyzed by methylsulfinyl carbanion in dimethyl sulfoxide. *Journal of Biochemistry*, *55*, 205–208.

Ho, Y. S., Yu, M. S., Yang, X. F., So, K. F., Yuen, W. H., & Chang, R. C. (2010). Neuroprotective effects of polysaccharides from wolfberry, the fruits of *Lycium barbarum*, against homocysteine-induced toxicity in rat cortical neurons. *Journal of Alzheimer's Disease*, *19*, 813–827.

Hu, J., Geng, M., Li, J., Xin, X., Wang, J., Tang, M., et al. (2004). Acidic oligosaccharide sugar chain, a marine-derived acidic oligosaccharide, inhibits the cytotoxicity and aggregation of amyloid beta protein. *Journal of Pharmacological Sciences*, *95*, 248–255.

Ittner, L. M., & Gotz, J. (2011). Amyloid-β and tau – A toxic pas de deux in Alzheimer's disease. *Nature Reviews. Neuroscience*, *12*, 65–72.

Kwon, S.-H., Hong, S.-I., Kim, J.-A., Jung, Y.-H., Kim, S.-Y., Kim, H.-C., et al. (2011). The neuroprotective effects of *Lonicera japonica* Thunb. against hydrogen peroxide-induced apoptosis via phosphorylation of MAPKs and PI3K/Akt in SH-SY5Y cells. *Food and Chemical Toxicology*, *49*, 1011–1019.

Lesne, S., Koh, M. T., Kotilinek, L., Kayed, R., Glabe, C. G., Yang, A., et al. (2006). A specific amyloid-beta protein assembly in the brain impairs memory. *Nature*, *440*, 352–357.

Liu, C., Sawaya, M. R., Cheng, P. N., Zheng, J., Nowick, J. S., & Eisenberg, D. (2011). Characteristics of amyloid-related oligomers revealed by crystal structures of macrocyclic beta-sheet mimics. *Journal of the Americal Chemical Society*, *133*, 6736–6744.

Lowry, O. H., Rosebrough, N. J., Farr, A. L., & Randall, R. J. (1951). Protein measurement with the Folin phenol reagent. *Journal of Biological Chemistry*, *193*, 265–275.

Matveeva, E. G., Rudolph, A., Moll, J. R., & Thompson, R. B. (2012). Structure-selective anisotropy assay for amyloid beta oligomers. *ACS Chemical Neuroscience*, *3*, 982–987.

McKoy, A. F., Chen, J., Schupbach, T., & Hecht, M. H. (2012). A novel inhibitor of amyloid β (Aβ) peptide aggregation: From high throughput screening to efficacy in an animal model of Alzheimer disease. *Journal of Biological Chemistry*, *287*, 38992–39000.

Nathalie, P., & Jean-Noel, O. (2008). Processing of amyloid precursor protein and amyloid peptide neurotoxicity. *Current Alzheimer Research*, *5*, 92–99.

Ono, K., Condron, M. M., & Teplow, D. B. (2009). Structure–neurotoxicity relationships of amyloid beta-protein oligomers. *Proceedings of the National Academy of Sciences of the United States of America*, *106*, 14745–14750.

Prasansuklab, A., & Tencomnao, T. (2013). Amyloidosis in Alzheimer's Disease: The toxicity of amyloid beta (Aβ), mechanisms of its accumulation and implications of medicinal plants for therapy. *Evidencebased Complementary Alternative Medicine*, *2013*, 413808.

Salminen, A., Ojala, J., Kauppinen, A., Kaarniranta, K., & Suuronen, T. (2009). Inflammation in Alzheimer's disease: Amyloid-beta oligomers trigger innate immunity defence via pattern recognition receptors. *Progress in Neurobiology*, *87*, 181–194.

Selkoe, D. J. (1997). Alzheimer's disease: Genotypes, phenotypes, and treatments. *Science*, *275*, 630–631.

Shang, X., Pan, H., Li, M., Miao, X., & Ding, H. (2011). *Lonicera japonica* Thunb.: Ethnopharmacology, phytochemistry and pharmacology of an important traditional Chinese medicine. *Journal of Ethnopharmacology*, *138*, 1–21.

Tseng, B. P., Green, K. N., Chan, J. L., Blurton-Jones, M., & LaFerla, F. M. (2008). Abeta inhibits the proteasome and enhances amyloid and tau accumulation. *Neurobiology of Aging*, *29*, 1607–1618.

Wada, M., Miyazawa, Y., & Miura, Y. (2011). A specific inhibitory effect of multivalent trehalose toward Aβ(1–40) aggregation. *Polymer Chemistry*, *2*, 1822.

Wang, P. P., Zhao, X. L., Lv, Y. J., Liu, Y. N., Lang, Y. Z., Wu, J. D., et al. (2012). Analysis of structural heterogeneity of fucoidan from *Hizikia fusiforme* by ES-CID-MS/MS. *Carbohydrate Polymers*, *90*, 602–607.

Wimo, A., Winblad, B., & Jonsson, L. (2010). The worldwide societal costs of dementia: Estimates for 2009. *Alzheimers Dementia*, *6*, 98–103.

Yankner, B. A. (1996). Mechanisms of neuronal degeneration in Alzheimer's disease. *Neuron*, *16*, 921–932.

Zheng, W. H., Bastianetto, S., Mennicken, F., Ma, W., & Kar, S. (2002). Amyloid beta peptide induces tau phosphorylation and loss of cholinergic neurons in rat primary septal cultures. *Neuroscience*, *115*, 201–211.